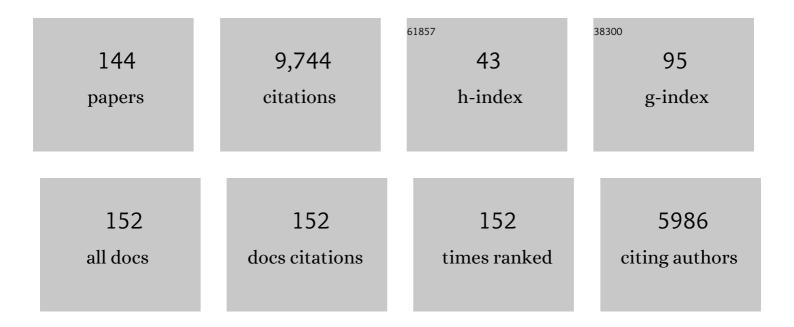
Moataz Attallah

List of Publications by Year in descending order

Source: https://exaly.com/author-pdf/5781689/publications.pdf Version: 2024-02-01



| # | Article | IF | CITATIONS |
|----|--|-----|-----------|
| 1 | Selective laser melting of AlSi10Mg alloy: Process optimisation and mechanical properties development. Materials & Design, 2015, 65, 417-424. | 5.1 | 866 |
| 2 | On the role of melt flow into the surface structure and porosity development during selective laser melting. Acta Materialia, 2015, 96, 72-79. | 3.8 | 715 |
| 3 | Microstructure and tensile properties of selectively laser-melted and of HIPed laser-melted Ti–6Al–4V. Materials Science & Engineering A: Structural Materials: Properties, Microstructure and Processing, 2013, 578, 230-239. | 2.6 | 613 |
| 4 | The influence of the laser scan strategy on grain structure and cracking behaviour in SLM powder-bed fabricated nickel superalloy. Journal of Alloys and Compounds, 2014, 615, 338-347. | 2.8 | 539 |
| 5 | Microstructural and texture development in direct laser fabricated IN718. Materials Characterization, 2014, 89, 102-111. | 1.9 | 420 |
| 6 | Microstructure and strength of selectively laser melted AlSi10Mg. Acta Materialia, 2016, 117, 311-320. | 3.8 | 380 |
| 7 | Fluid and particle dynamics in laser powder bed fusion. Acta Materialia, 2018, 142, 107-120. | 3.8 | 367 |
| 8 | Influence of processing conditions on strut structure and compressive properties of cellular lattice structures fabricated by selective laser melting. Materials Science & Engineering A: Structural Materials: Properties, Microstructure and Processing, 2015, 628, 188-197. | 2.6 | 289 |
| 9 | Fabrication of large Ti–6Al–4V structures by direct laser deposition. Journal of Alloys and Compounds, 2015, 629, 351-361. | 2.8 | 243 |
| 10 | Microstructure and yield strength of SLM-fabricated CM247LC Ni-Superalloy. Acta Materialia, 2017, 128, 87-95. | 3.8 | 242 |
| 11 | Selective laser melting of AlSi10Mg: Influence of post-processing on the microstructural and tensile properties development. Materials and Design, 2016, 105, 212-222. | 3.3 | 237 |
| 12 | The development of TiNi-based negative Poisson's ratio structure using selective laser melting. Acta Materialia, 2016, 105, 75-83. | 3.8 | 231 |
| 13 | Mesoscale modelling of selective laser melting: Thermal fluid dynamics and microstructural evolution. Computational Materials Science, 2017, 126, 479-490. | 1.4 | 227 |
| 14 | Additive manufacturing of Ni-based superalloys: The outstanding issues. MRS Bulletin, 2016, 41, 758-764. | 1.7 | 194 |
| 15 | Selective laser melting of Invar 36: Microstructure and properties. Acta Materialia, 2016, 103, 382-395. | 3.8 | 185 |
| 16 | On the role of thermal fluid dynamics into the evolution of porosity during selective laser melting. Scripta Materialia, 2015, 105, 14-17. | 2.6 | 172 |
| 17 | The barriers to the progression of additive manufacture: Perspectives from UK industry. International Journal of Production Economics, 2018, 198, 104-118. | 5.1 | 157 |
| 18 | Friction stir welding parameters: a tool for controlling abnormal grain growth during subsequent heat treatment. Materials Science & Engineering A: Structural Materials: Properties, Microstructure and Processing, 2005, 391, 51-59. | 2.6 | 154 |

| # | Article | IF | CITATIONS |
|----|--|-----|-----------|
| 19 | Process optimisation of selective laser melting using energy density model for nickel based superalloys. Materials Science and Technology, 2016, 32, 657-661. | 0.8 | 151 |
| 20 | Effect of the forging pressure on the microstructure and residual stress development in Ti–6Al–4V linear friction welds. Acta Materialia, 2009, 57, 5582-5592. | 3.8 | 128 |
| 21 | Influence of hot isostatic pressing temperature on microstructure and tensile properties of a nickel-based superalloy powder. Materials Science & Engineering A: Structural Materials: Properties, Microstructure and Processing, 2013, 564, 176-185. | 2.6 | 99 |
| 22 | Fabricating CoCrFeMnNi high entropy alloy via selective laser melting in-situ alloying. Journal of Materials Science and Technology, 2020, 43, 40-43. | 5.6 | 96 |
| 23 | Laser Powder Bed Fusion of Ti-rich TiNi lattice structures: Process optimisation, geometrical integrity, and phase transformations. International Journal of Machine Tools and Manufacture, 2019, 141, 19-29. | 6.2 | 93 |
| 24 | Linking microstructure and processing defects to mechanical properties of selectively laser melted AlSi10Mg alloy. Theoretical and Applied Fracture Mechanics, 2018, 98, 123-133. | 2.1 | 92 |
| 25 | The design of additively manufactured lattices to increase the functionality of medical implants. Materials Science and Engineering C, 2019, 94, 901-908. | 3.8 | 89 |
| 26 | Cracking during thermal post-processing of laser powder bed fabricated CM247LC Ni-superalloy. Materials and Design, 2019, 174, 107793. | 3.3 | 80 |
| 27 | Additive manufacturing of bio-inspired multi-scale hierarchically strengthened lattice structures. International Journal of Machine Tools and Manufacture, 2021, 167, 103764. | 6.2 | 74 |
| 28 | Microstructural control during direct laser deposition of a Î ² -titanium alloy. Materials & Design, 2015, 81, 21-30. | 5.1 | 70 |
| 29 | In-situ alloyed, oxide-dispersion-strengthened CoCrFeMnNi high entropy alloy fabricated via laser powder bed fusion. Materials and Design, 2020, 194, 108966. | 3.3 | 69 |
| 30 | Selective Laser Melting of Ti-6Al-4V: The Impact of Post-processing on the Tensile, Fatigue and Biological Properties for Medical Implant Applications. Materials, 2020, 13, 2813. | 1.3 | 69 |
| 31 | Optimisation of selective laser melting for a high temperature Ni-superalloy. Rapid Prototyping Journal, 2015, 21, 423-432. | 1.6 | 68 |
| 32 | Adding functionality with additive manufacturing: Fabrication of titanium-based antibiotic eluting implants. Materials Science and Engineering C, 2016, 64, 407-415. | 3.8 | 67 |
| 33 | Development and testing of an additively manufactured monolithic catalyst bed for HTP thruster applications. Applied Catalysis A: General, 2017, 542, 125-135. | 2.2 | 64 |
| 34 | Influence of processing parameters on internal porosity and types of defects formed in Ti6Al4V lattice structure fabricated by selective laser melting. Materials Science & Engineering A: Structural Materials: Properties, Microstructure and Processing, 2019, 767, 138387. | 2.6 | 58 |
| 35 | Laser powder bed fusion in high-pressure atmospheres. International Journal of Advanced Manufacturing Technology, 2018, 99, 543-555. | 1.5 | 56 |
| 36 | Direct laser fabrication of three dimensional components using SC420 stainless steel. Materials & Design, 2013, 47, 731-736. | 5.1 | 55 |

| # | Article | IF | CITATIONS |
|----|---|-----|-----------|
| 37 | Compressive behavior of stretched and composite microlattice metamaterial for energy absorption applications. Composites Part B: Engineering, 2020, 184, 107715. | 5.9 | 51 |
| 38 | Evolution of grain boundary network topology in 316L austenitic stainless steel during powder hot isostatic pressing. Acta Materialia, 2017, 133, 269-281. | 3.8 | 50 |
| 39 | Controlling the grain orientation during laser powder bed fusion to tailor the magnetic characteristics in a Ni-Fe based soft magnet. Acta Materialia, 2018, 158, 230-238. | 3.8 | 49 |
| 40 | Laser powder bed fusion at sub-atmospheric pressures. International Journal of Machine Tools and Manufacture, 2018, 130-131, 65-72. | 6.2 | 47 |
| 41 | Porosity control in 316L stainless steel using cold and hot isostatic pressing. Materials and Design, 2018, 138, 21-29. | 3.3 | 47 |
| 42 | Assessment of trapped powder removal and inspection strategies for powder bed fusion techniques. International Journal of Advanced Manufacturing Technology, 2020, 106, 4521-4532. | 1.5 | 47 |
| 43 | Machining and heat treatment as post-processing strategies for Ni-superalloys structures fabricated using direct energy deposition. Journal of Manufacturing Processes, 2021, 61, 236-244. | 2.8 | 47 |
| 44 | Tailoring selective laser melting process for titanium drug-delivering implants with releasing micro-channels. Additive Manufacturing, 2018, 20, 144-155. | 1.7 | 45 |
| 45 | Classifying shape of internal pores within AlSi10Mg alloy manufactured by laser powder bed fusion using 3D X-ray micro computed tomography: Influence of processing parameters and heat treatment. Materials Characterization, 2020, 163, 110225. | 1.9 | 45 |
| 46 | Influence of the kissing bond on the mechanical properties and fracture behaviour of AA5083-H112 friction stir welds. Materials Science & Engineering A: Structural Materials: Properties, Microstructure and Processing, 2018, 719, 12-20. | 2.6 | 44 |
| 47 | Comparative determination of the $\hat{l}\pm/\hat{l}^2$ phase fraction in $\hat{l}\pm+\hat{l}^2$ -titanium alloys using X-ray diffraction and electron microscopy. Materials Characterization, 2009, 60, 1248-1256. | 1.9 | 43 |
| 48 | Effect of grain size reduction of AA2124 aluminum alloy powder compacted by spark plasma sintering. Journal of Alloys and Compounds, 2014, 609, 215-221. | 2.8 | 42 |
| 49 | Deformation mechanisms of FeCoCrNiMo0.2 high entropy alloy at 77 and 15ÂK. Scripta Materialia, 2020, 178, 166-170. | 2.6 | 41 |
| 50 | Surface Finish has a Critical Influence on Biofilm Formation and Mammalian Cell Attachment to Additively Manufactured Prosthetics. ACS Biomaterials Science and Engineering, 2017, 3, 1616-1626. | 2.6 | 40 |
| 51 | Effect of powder characteristics and oxygen content on modifications to the microstructural topology during hot isostatic pressing of an austenitic steel. Acta Materialia, 2019, 172, 6-17. | 3.8 | 39 |
| 52 | Microstructural control in a Ti-based alloy by changing laser processing mode and power during direct laser deposition. Materials Letters, 2016, 179, 104-108. | 1.3 | 36 |
| 53 | Influence of powder characteristics on the microstructure and mechanical properties of HIPped CM247LC Ni superalloy. Materials and Design, 2019, 174, 107796. | 3.3 | 35 |
| 54 | In-situ alloying of AlSi10Mg+Si using Selective Laser Melting to control the coefficient of thermal expansion. Journal of Alloys and Compounds, 2019, 795, 8-18. | 2.8 | 35 |

| # | Article | IF | CITATIONS |
|----|--|-----|-----------|
| 55 | Additive manufacturing of a topology-optimised multi-tube energy storage device: Experimental tests and numerical analysis. Applied Thermal Engineering, 2020, 180, 115878. | 3.0 | 35 |
| 56 | Influence of base metal microstructure on microstructural development in aluminium based alloy friction stir welds. Science and Technology of Welding and Joining, 2007, 12, 361-369. | 1.5 | 34 |
| 57 | Net-shape manufacturing using hybrid selective laser melting/hot isostatic pressing. Rapid Prototyping Journal, 2017, 23, 720-726. | 1.6 | 34 |
| 58 | Laser powder bed fusion of a Zr-alloy: Tensile properties and biocompatibility. Materials Letters, 2020, 259, 126897. | 1.3 | 34 |
| 59 | Deformation of microstructurally refined cast Ti46Al8Nb and Ti46Al8Ta. Intermetallics, 2012, 23, 1-11. | 1.8 | 32 |
| 60 | In-situ shelling via selective laser melting: Modelling and microstructural characterisation. Materials and Design, 2015, 87, 845-853. | 3.3 | 31 |
| 61 | 3-D Printed Slotted Spherical Resonator Bandpass Filters With Spurious Suppression. IEEE Access, 2019, 7, 128026-128034. | 2.6 | 29 |
| 62 | Characterization of Dissimilar Linear Friction Welds of $\hat{I}\pm\cdot\hat{I}^2$ Titanium Alloys. Journal of Materials Engineering and Performance, 2012, 21, 770-776. | 1.2 | 28 |
| 63 | Fracture of three-dimensional lattices manufactured by selective laser melting. International Journal of Solids and Structures, 2019, 180-181, 147-159. | 1.3 | 28 |
| 64 | Microstructure-microhardness relationships in friction stir welded AA5251. Journal of Materials Science, 2007, 42, 7299-7306. | 1.7 | 27 |
| 65 | In-Situ observation of primary $\hat{I}^3 \hat{a} \in 2$ melting in Ni-base superalloy using confocal laser scanning microscopy. Materials Characterization, 2011, 62, 760-767. | 1.9 | 27 |
| 66 | Linear friction welding of Ti6Al4V: Experiments and modelling. Materials Science and Technology, 2015, 31, 372-384. | 0.8 | 26 |
| 67 | A new approach to develop palladium-modified Ti-based alloys for biomedical applications. Materials and Design, 2016, 109, 98-111. | 3.3 | 26 |
| 68 | Influence of the heating rate on the initiation of primary recrystallization in a deformed Al–Mg alloy. Scripta Materialia, 2010, 63, 371-374. | 2.6 | 25 |
| 69 | An iterative approach of hot isostatic pressing tooling design for net-shape IN718 superalloy parts. International Journal of Advanced Manufacturing Technology, 2016, 83, 1835-1845. | 1.5 | 25 |
| 70 | Microstructural Development and Mechanical Properties of Friction Stir Welded Ferritic Stainless Steel AISI 409. Journal of Materials Engineering and Performance, 2019, 28, 6391-6406. | 1.2 | 25 |
| 71 | Evolution of internal pores within AlSi10Mg manufactured by laser powder bed fusion under tension: As-built and heat treated conditions. Materials and Design, 2021, 204, 109645. | 3.3 | 25 |
| 72 | Controlling microstructural and mechanical properties of direct laser deposited Inconel 718 via laser power. Journal of Alloys and Compounds, 2021, 872, 159588. | 2.8 | 25 |

| # | Article | IF | CITATIONS |
|----|---|-----|-----------|
| 73 | Additive manufacturing of magnetic shielding and ultra-high vacuum flange for cold atom sensors. Scientific Reports, 2018, 8, 2023. | 1.6 | 24 |
| 74 | Microstructural and Mechanical Characterization of Thin-Walled Tube Manufactured with Selective Laser Melting for Stent Application. Journal of Materials Engineering and Performance, 2021, 30, 696-710. | 1.2 | 24 |
| 75 | Development, characterisation, and modelling of processability of nitinol stents using laser powder bed fusion. Journal of Alloys and Compounds, 2022, 909, 164681. | 2.8 | 24 |
| 76 | Experimental and numerical investigations on the process quality and microstructure during induction heating assisted incremental forming of Ti-6Al-4V sheet. Journal of Materials Processing Technology, 2022, 299, 117323. | 3.1 | 22 |
| 77 | The Effect of Powder Characteristics on Build Quality of High-Purity Tungsten Produced via Laser Powder Bed Fusion (LPBF). Metallurgical and Materials Transactions A: Physical Metallurgy and Materials Science, 2020, 51, 1367-1378. | 1.1 | 21 |
| 78 | In situ alloying based laser powder bed fusion processing of β Ti–Mo alloy to fabricate functionally graded composites. Composites Part B: Engineering, 2021, 222, 109059. | 5.9 | 21 |
| 79 | Development of Ni-base metal matrix composites by powder metallurgy hot isostatic pressing for space applications. Advanced Powder Technology, 2022, 33, 103411. | 2.0 | 21 |
| 80 | Microstructural and Residual Stress Development due to Inertia Friction Welding in Ti-6246. Metallurgical and Materials Transactions A: Physical Metallurgy and Materials Science, 2012, 43, 3149-3161. | 1.1 | 20 |
| 81 | Finite Element Modeling of the Inertia Friction Welding of Dissimilar High-Strength Steels. Metallurgical and Materials Transactions A: Physical Metallurgy and Materials Science, 2013, 44, 5054-5064. | 1.1 | 20 |
| 82 | Post Processing of 3D Printed Metal Scaffolds: a Preliminary Study of Antimicrobial Efficiency. Procedia Manufacturing, 2020, 47, 1106-1112. | 1.9 | 20 |
| 83 | The effect of the heat treatments on the tool wear of hybrid Additive Manufacturing of IN718. Wear, 2021, 470-471, 203617. | 1.5 | 20 |
| 84 | Inertia friction welding (IFW) for aerospace applications. , 2012, , 25-74. | | 18 |
| 85 | Rheological characterization and shape control in gel-casting of nano-sized zirconia powders. Ceramics International, 2014, 40, 14405-14412. | 2.3 | 18 |
| 86 | Influence of the laser source pulsing frequency on the direct laser deposited Inconel 718 thin walls. Journal of Alloys and Compounds, 2021, 856, 158095. | 2.8 | 18 |
| 87 | Direct laser deposition of crack-free CM247LC thin walls: Mechanical properties and microstructural effects of heat treatment. Materials and Design, 2021, 211, 110123. | 3.3 | 18 |
| 88 | Microstructural control during laser powder fusion to create graded microstructure Ni-superalloy components. Additive Manufacturing, 2020, 36, 101432. | 1.7 | 16 |
| 89 | SLM Printed Waveguide Dual-Mode Filters With Reduced Sensitivity to Fabrication Imperfections. IEEE Microwave and Wireless Components Letters, 2021, 31, 1195-1198. | 2.0 | 16 |
| 90 | The influence of zirconium content on the microstructure, mechanical properties, and biocompatibility of in-situ alloying Ti-Nb-Ta based β alloys processed by selective laser melting. Materials Science and Engineering C, 2021, 131, 112486. | 3.8 | 16 |

| # | Article | IF | CITATIONS |
|-----|---|-----|-----------|
| 91 | In situ neutron diffraction unravels deformation mechanisms of a strong and ductile FeCrNi medium entropy alloy. Journal of Materials Science and Technology, 2022, 116, 103-120. | 5.6 | 16 |
| 92 | Spatial variation of microtexture in linear friction welded Ti-6Al-4V. Materials Characterization, 2017, 127, 342-347. | 1.9 | 15 |
| 93 | A Convolutional Neural Network (CNN) classification to identify the presence of pores in powder bed fusion images. International Journal of Advanced Manufacturing Technology, 2022, 120, 5133-5150. | 1.5 | 15 |
| 94 | Validation of a Model of Linear Friction Welding of Ti6Al4V by Considering Welds of Different Sizes. Metallurgical and Materials Transactions B: Process Metallurgy and Materials Processing Science, 2015, 46, 2326-2331. | 1.0 | 14 |
| 95 | Effect of Microstructure on the Morphology of Atmospheric Corrosion Pits in Type 304L Stainless Steel. Corrosion, 2018, 74, 1373-1384. | 0.5 | 14 |
| 96 | The role of powder atomisation route on the microstructure and mechanical properties of hot isostatically pressed Inconel 625. Materials Science & Engineering A: Structural Materials: Properties, Microstructure and Processing, 2021, 808, 140950. | 2.6 | 13 |
| 97 | A synchrotron tomographic energy-dispersive diffraction imaging study of the aerospace alloy Ti 6246. Journal of Applied Crystallography, 2011, 44, 150-157. | 1.9 | 12 |
| 98 | Gel casting of sialon ceramics based on water soluble epoxy resin. Ceramics International, 2015, 41, 11534-11538. | 2.3 | 12 |
| 99 | Laser Powder Bed Fusion of Ti-6Al-2Sn-4Zr-6Mo Alloy and Properties Prediction Using Deep Learning Approaches. Materials, 2021, 14, 2056. | 1.3 | 12 |
| 100 | A 3-D Printed 300 GHz Waveguide Cavity Filter by Micro Laser Sintering. IEEE Transactions on Terahertz Science and Technology, 2022, 12, 274-281. | 2.0 | 12 |
| 101 | Influence of process parameters on superplasticity of friction stir processed nugget in high strength Al – Cu – Li alloy. Materials Science and Technology, 2004, 20, 1370-1376. | 0.8 | 10 |
| 102 | Shaping and Slotting High-Q Spherical Resonators for Suppression of Higher Order Modes. , 2019, , . | | 10 |
| 103 | Novel Hybrid Manufacturing Process of CM247LC and Multi-Material Blisks. Micromachines, 2020, 11, 492. | 1.4 | 10 |
| 104 | Magnetic shielding promotion via the control of magnetic anisotropy and thermal Post processing in laser powder bed fusion processed NiFeMo-based soft magnet. Additive Manufacturing, 2020, 32, 101079. | 1.7 | 9 |
| 105 | Microstructure-magnetic shielding development in additively manufactured Ni-Fe-Mo soft magnet alloy in the as fabricated and post-processed conditions. Journal of Alloys and Compounds, 2021, 884, 161112. | 2.8 | 9 |
| 106 | Monolithic 3Dâ€printed slotted hemisphere resonator bandpass filter with extended spuriousâ€free stopband. Electronics Letters, 2019, 55, 331-333. | 0.5 | 8 |
| 107 | Synchrotron Characterisation of Ultra-Fine Grain TiB2/Al-Cu Composite Fabricated by Laser Powder Bed Fusion. Acta Metallurgica Sinica (English Letters), 2022, 35, 78-92. | 1.5 | 8 |
| 108 | A Narrowband 3-D Printed Invar Spherical Dual-Mode Filter With High Thermal Stability for OMUXs. IEEE Transactions on Microwave Theory and Techniques, 2022, 70, 2165-2173. | 2.9 | 8 |

| # | Article | IF | CITATIONS |
|-----|--|-----|-----------|
| 109 | Finite Element Modeling of Machining Nickel Superalloy Produced By Direct Energy Deposition Process. Procedia Manufacturing, 2020, 47, 525-529. | 1.9 | 7 |
| 110 | Microstructural characterisation and high-temperature oxidation of laser powder bed fusion processed Inconel 625. Materials Letters, 2022, 311, 131582. | 1.3 | 7 |
| 111 | Powder HIP of pure Nb and C-103 alloy: The influence of powder characteristics on mechanical properties. International Journal of Refractory Metals and Hard Materials, 2022, 104, 105803. | 1.7 | 7 |
| 112 | Neural Network Modeling of NiTiHf Shape Memory Alloy Transformation Temperatures. Journal of Materials Engineering and Performance, 2022, 31, 10258-10270. | 1.2 | 7 |
| 113 | Netshape centrifugal gel-casting of high-temperature sialon ceramics. Ceramics International, 2018, 44, 3440-3447. | 2.3 | 6 |
| 114 | Monolithic 3D printed waveguide filters with wide spuriousâ€free stopbands using dimpled spherical resonators. IET Microwaves, Antennas and Propagation, 2021, 15, 1657-1670. | 0.7 | 6 |
| 115 | A Melt Pool Temperature Model in Laser Powder Bed Fabricated CM247LC Ni Superalloy to Rationalize Crack Formation and Microstructural Inhomogeneities. Metallurgical and Materials Transactions A: Physical Metallurgy and Materials Science, 2021, 52, 5221-5234. | 1.1 | 6 |
| 116 | In-situ alloyed CoCrFeMnNi high entropy alloy: Microstructural development in laser powder bed fusion. Journal of Materials Science and Technology, 2022, 123, 123-135. | 5.6 | 6 |
| 117 | Microstructural Evolution, Mechanical Properties, and Preosteoblast Cell Response of a Post-Processing-Treated TNT5Zr β Ti Alloy Manufactured via Selective Laser Melting. ACS Biomaterials Science and Engineering, 2022, 8, 2336-2348. | 2.6 | 6 |
| 118 | Suspended dropletÂalloying: A new method for combinatorial alloy synthesis; nitinol-based alloys as an example. Journal of Alloys and Compounds, 2018, 768, 392-398. | 2.8 | 5 |
| 119 | The analogies between human development and additive manufacture: Expanding the definition of design. Cogent Engineering, 2019, 6, . | 1.1 | 5 |
| 120 | A high strength and low modulus metastable β Ti-12Mo-6Zr-2Fe alloy fabricated by laser powder bed fusion in-situ alloying. Additive Manufacturing, 2021, 37, 101708. | 1.7 | 5 |
| 121 | Revealing the microstructural evolution of electron beam powder bed fusion and hot isostatic pressing Ti-6Al-4V in-situ shelling samples using X-ray computed tomography. Additive Manufacturing, 2022, 57, 102962. | 1.7 | 5 |
| 122 | Composite Powder Consolidation Using Selective Laser Melting: Input Energy/Porosity Morphology/Balling Effect Relation. Minerals, Metals and Materials Series, 2017, , 169-180. | 0.3 | 4 |
| 123 | Comparison of LPBF processing of AlSi40 alloy using blended and pre-alloyed powder. Additive Manufacturing Letters, 2022, 2, 100038. | 0.9 | 4 |
| 124 | Influence of the microstructural inhomogeneities on the martensite-to-austenite phase transformation temperatures in TiNiCu-based shape-memory alloys. Materials Chemistry and Physics, 2013, 141, 272-277. | 2.0 | 3 |
| 125 | On the constitutive relationship between solidification cells and the fatigue behaviour of IN718 fabricated by laser powder bed fusion. Additive Manufacturing, 2021, 47, 102347. | 1.7 | 3 |
| 126 | The influence of advanced hot isostatic pressing on phase transformations, mechanical properties of Ti-34Nb-13Ta-5Zr-0.2O alloy manufactured by In-situ alloying via selective laser melting. Journal of Alloys and Compounds, 2022, 903, 163974. | 2.8 | 3 |

| # | Article | IF | CITATIONS |
|-----|---|-----|-----------|
| 127 | Thermal Stability Analysis of 3D Printed Resonators Using Novel Materials. , 2022, , . | | 3 |
| 128 | In-vitro Study of Effect of the Design of the Stent on the Arterial Waveforms. Procedia Structural Integrity, 2019, 15, 33-40. | 0.3 | 2 |
| 129 | Metal 3D Printed D-Band Waveguide to Surface Wave Transition. , 2020, , . | | 2 |
| 130 | Hybrid Electron Beam Powder Bed Fusion Additive Manufacturing of Ti–6Al–4V: Processing, Microstructure, and Mechanical Properties. Metallurgical and Materials Transactions A: Physical Metallurgy and Materials Science, 2022, 53, 927-941. | 1.1 | 2 |
| 131 | Friction welding of titanium alloys: addressing the structural integrity issues through process optimisation. , 2013, , 313-315. | | 1 |
| 132 | New materials development. , 2021, , 529-562. | | 1 |
| 133 | Design of a Metal 3-D Printed Corrugated Antenna. , 2019, , . | | 1 |
| 134 | Deformation of AlSi10Mg parts manufactured by Laser Powder Bed Fusion: In-situ measurements incorporating X-ray micro computed tomography and a micro testing stage. Procedia Structural Integrity, 2022, 35, 168-172. | 0.3 | 1 |
| 135 | Temperature-dependent enthalpy and entropy stabilization of solid solution phases in non-equiatomic CoCrFeNiTi high entropy alloys: computational phase diagrams and thermodynamics. Modelling and Simulation in Materials Science and Engineering, 2022, 30, 045013. | 0.8 | 1 |
| 136 | Influence of Forging Pressure on Microstructural and Mechanical Properties Development in Linear Friction Welded Al-Cu Dissimilar Joint. Soldagem E Inspecao, 0, 24, . | 0.6 | 0 |
| 137 | Stereological Analysis of the Microstructural Inhomogeneities in Direct-Chill Cast and Continuous-Cast Aluminium-Magnesium Alloy (AA5754). Praktische Metallographie/Practical Metallography, 2014, 51, 77-94. | 0.1 | 0 |
| 138 | Making the most of additive layer manufacture - development of tailored titanium implants with embedded therapeutics. Frontiers in Bioengineering and Biotechnology, 0, 4, . | 2.0 | 0 |
| 139 | The Influence of Processing Parameters on Strut Diameter and Internal Porosity in Ti6Al4V Cellular Structure. , 2018, , . | | Ο |
| 140 | Phase Diagram and Mechanical Properties of a CoCrFeNi1??Ti? High Entropy Alloy Fabricated by Mechanical Alloying. , 2019, , . | | 0 |
| 141 | Effect of Stoichiometry on Shape Memory Properties of Ti-Ni-Hf-Cu-Nb Shape Memory Alloys Manufactured by Suspended Droplet Alloying. Solids, 2022, 3, 1-21. | 1.1 | О |
| 142 | Microstructure, tensile properties of SLMed TNT5Zr-0.2O alloys without/with keyholes produced by different Post-processing treatments. Materials Letters, 2022, 309, 131448. | 1.3 | 0 |
| 143 | Enabling high efficiency magnetic refrigeration using laser powder bed fusion of porous LaCe(Fe,Mn,Si)13 structures. Additive Manufacturing, 2022, 51, 102620. | 1.7 | 0 |
| 144 | Effect of Oxygen Diffusion During the Post-Processing of Ti6Al4V Lattice Structures Fabricated by the Selective Laser Melting Process. Journal of Engineering Materials and Technology, Transactions of the ASME, 2022, 144, . | 0.8 | 0 |